Liquid Crystals
Publication details, including instructions for authors and subscription information:
http://www.informaworld.com/smpp/title~content=t713926090

Thermotropic liquid crystal behaviour of gemini imidazolium-based ionic amphiphiles

Jason E. Bara[ab]; Evan S. Hatakeyama[a]; Brian R. Wiesenauer[b]; Xiaohui Zeng[b]; Richard D. Noble[a]; Douglas L. Gin[ab]
[a] Department of Chemical and Biological Engineering, University of Colorado at Boulder, Boulder, CO, USA [b] Department of Chemistry and Biochemistry, University of Colorado at Boulder, Boulder, CO, USA

Online publication date: 10 December 2010

To cite this Article Bara, Jason E. , Hatakeyama, Evan S. , Wiesenauer, Brian R. , Zeng, Xiaohui , Noble, Richard D. and Gin, Douglas L.(2010) 'Thermotropic liquid crystal behaviour of gemini imidazolium-based ionic amphiphiles', Liquid Crystals, 37: 12, 1587 — 1599
To link to this Article: DOI: 10.1080/02678292.2010.521859
URL: http://dx.doi.org/10.1080/02678292.2010.521859

Liquid Crystals,
Vol. 37, No. 12, December 2010, 1587–1599

Taylor & Francis
Taylor & Francis Group

Thermotropic liquid crystal behaviour of gemini imidazolium-based ionic amphiphiles

Jason E. Bara[a,b†], Evan S. Hatakeyama[a], Brian R. Wiesenauer[b], Xiaohui Zeng[b], Richard D. Noble[a] and Douglas L. Gin[a,b]*

[a]*Department of Chemical and Biological Engineering, University of Colorado at Boulder, Boulder, CO, USA;* [b]*Department of Chemistry and Biochemistry, University of Colorado at Boulder, Boulder, CO, USA*

(*Received 4 April 2010; final version received 3 September 2010*)

Thermotropic ionic liquid crystals (LCs) are useful for a number of applications such as anisotropic ion transport and as organised reaction media/solvents because of their ordered fluid properties and intrinsic charge units. A large number of different ionic LC architectures are known, but only a handful of examples of gemini (i.e. paired or dimeric) ionic LCs have been prepared and studied. In this work, a series of 20 new symmetric, imidazolium-based, gemini cationic LCs containing two bridged imidazolium cations and two pendant alkyl chains was synthesised, and the thermotropic LC behaviours were characterised. The imidazolium unit provides a highly tunable and modular platform for the design and synthesis of gemini cationic LCs which offers excellent structure control. As expected, the thermotropic LC properties of these new amphilphilic, gemini ionic LCs were found to be strongly influenced by the length of the spacer between the imidazolium units, the length of the pendant alkyl tails, and the nature of the anion. Smectic A (SmA) thermotropic LC phases were observed in more than half of the gemini imidazolium LC systems studied.

Keywords: gemini imidazolium salts; thermotropic ionic liquid crystals; synthesis of imidazole derivatives; nanostructured materials; smectic phases

1. Introduction

Ionic liquid crystals (LCs) are a special class of mesogenic compounds that contain intrinsic cationic and/or anionic components (for a comprehensive review on ionic LCs, see [1]). Like traditional non-charged LCs, ionic LCs self-organise into fluid assemblies that have varying degrees of average orientational order, resulting in the formation of distinct LC phases [1].

Thermotropic ionic LCs have recently been highlighted as a very important and unique subclass of ionic LCs because of their structural relationship and similarity with ionic liquids (ILs) [1]. ILs are molten organic salts at ambient temperature or below 100°C with negligible vapour pressure, and have found broad utility as new solvents for reactions, intrinsically ion-conducting fluids and new gas processing media (an overview of ionic liquids can be found in [2]). In addition to their similarity and potential ability to interface with ILs, thermotropic ionic LC assemblies have also found utility on their own as anisotropic ion-conductors and ordered reaction media that can perturb product selectivity values compared to conventional solvents [2].

A large range of different thermotropic ionic LC architectures and shapes have been prepared and explored in terms of their LC phase properties [1]. However, one ionic LC architecture that has been relatively unexplored with respect to thermotropic LC behaviour is the amphiphilic, gemini (i.e. dimeric) LC platform. Gemini amphiphilic molecules are a unique class of materials that typically contain two tethered hydrophilic (typically ionic) headgroups, each with one long pendant tail (Figure 1) [3, 4]. When used as surfactants, gemini amphiphiles are more stable and exhibit lower critical micelle concentrations (CMCs) than traditional single head group/single tail (i.e. monomeric) surfactants [3, 4].

We wish to note at this point that gemini imidazolium salts have also been called 'geminal' in several works [5–8]. The term 'geminal' is typically reserved to describe two identical functional groups attached to a single atom (i.e. a 'geminal diol'). The term 'gemini' is a more technically accurate description for two tethered imidazolium cations, as it implies a binary or 'twin' system, and is consistent with the terms originating in the surfactant literature [3].

Although the fundamental aqueous interfacial and self-assembly properties of amphiphilic gemini molecules compared to monomeric amphiphiles have been extensively studied [3, 4, 9–11], the thermotropic LC behaviour of these unique ionic molecules in their pure forms has been relatively unexplored with the exception of a small series of

†Current address: Department of Chemical and Biological Engineering, University of Alabama, Tuscaloosa, AL, USA

*Corresponding author. Email: douglas.gin@colorado.edu

ISSN 0267-8292 print/ISSN 1366-5855 online

DOI: 10.1080/02678292.2010.521859
http://www.informaworld.com

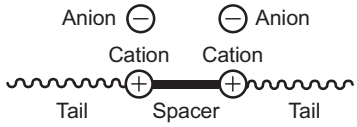

Figure 1. Depiction of the general structure of a cationic gemini amphiphile.

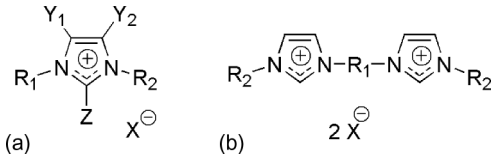

Figure 2. (a) Structure of an imidazolium salt and (b) general structure of gemini imidazolium amphiphiles synthesised in this work.

quaternary ammonium-based gemini amphiphiles in their pure states [4, 9–11]. Typically, these gemini ammonium amphiphilic LCs exhibit lamellar-type non-tilted smectic A (SmA) or tilted smectic C (SmC) bilayer type thermotropic LC phases [4, 9–11].

Imidazolium salts (Figure 2(a)) provide a highly tunable and modular platform for the design and synthesis of new ionic LC materials [1]. The imidazolium platform is amenable to the synthesis of gemini ILs, polymeric materials [5–8, 12–18], and LCs, the general structures of which are shown below (Figure 2(b)).

As illustrated in Figure 2(a), imidazolium-based cationic units offer exceptional control over structure and functionality, especially compared with the typical ammonium-based or phosphonium-based units commonly used to introduce organic cationic sites into surfactants and ionic polymers [1, 3]. For instance, the five-membered imidazolium ring can be selectively tailored/substituted at each of the N and C positions (Figure 2(a)) [2], and the anion can also be chosen from a wide range of species [2]. Many imidazole derivatives with various functional groups are commercially available and many more can be conveniently synthesised.

There have been only a few types of imidazolium-based LCs reported to date, with Kato and co-workers as the leaders in the design of imidazolium-containing ionic LC architectures. These imidazolium LCs have exhibited promising properties as anisotropic ion conductors [19–27]. The majority of these systems have been composed of an amphiphile consisting of a single imidazolium cation tethered to a bulky hydrocarbon component with a 'free' anion, and have exhibited either SmA or columnar hexagonal (Col_H) phases. Some of the reported systems were capable of interfacing with ILs. The Kato group has also reported a cationic LC system where a 'free' imidazolium cation was paired with an amphiphilic dodecylsulphonate anion [26]. Other work with imidazolium-based LCs has focused on forming new LC imidazolium salts [28–31] and tethering imidazolium cations to mesogenic groups [32] and rigid cores [33–35]. Polymerisation of imidazolium-based amphiphiles in the presence of water has been shown to result in LC hydrogels [36, 37]. Benzimidazolium cations have also been used as the central building block for synthesising novel LCs [38].

Only a very small number of examples of gemini imidazolium-based amphiphiles and their self-assembly properties have been reported in the literature. For example, a simple system wherein $R_1 = n$-C_4H_8, $R_2 = n$-$C_{14}H_{29}$ and X = Br (see Figure 2(b)) was shown to be more thermally stable and have a lower CMC than an analogous single-headed imidazolium amphiphile [14]. Another paper described a gemini imidazolium amphiphile where a linear n-$C_{17}H_{35}$ unit was present at the C(2) position with $R_2 = C_2H_5$, X = Br and R_1 as various lengths of n-alkyl spacers (see Figure 2(b)) [39]. In this latter work, the authors claimed that the method by which the gemini imidazolium salts were synthesised determined which nitrogen atom on the imidazolium ring held the cationic charge (i.e. those gemini imidazolium systems which were synthesised by bridging two imidazoles through quaternisation with a dibromoalkane were deemed 'exo' and those which were produced by quaternising both sides of a bis(imidazole) with bromoethane were deemed 'endo') [39]. However, this supposition is incorrect since it is well-known that the positive charge is substantially delocalised over the N(1), C(2) and N(3) positions of an imidazolium ring in an allyl cation type structure, and that its location is independent of the order or reaction [2]. Upon examination of their ^{1}H NMR data [40], the so-called 'endo' and 'exo' gemini imidazolium salts appear to be the same compounds, and the phenomena reported in that manuscript appear questionable.

Thus, with only a very small amount of basic data reported on gemini imidazolium LC salts, ample opportunities exist to probe the fundamental properties and characteristics of these materials. To understand how these dicationic systems may form LC phases in their neat states, we have synthesised a library of 20 symmetrical gemini imidazolium amphiphiles of the general structure shown in Figure 2(b) and studied their thermotropic LC behaviour. Structural variables encompassed the nature of the headgroup spacer, i.e. alkyl (C_n) or oligo(ethylene glycol) (PEG_p), spacer length (number of repeat units), anion type (Br^- or BF_4^-), and tail length (n-decyl, n-dodecyl and n-tetradecyl). The headgroup spacer was observed to have the

greatest effect on the ability to exhibit thermotropic LC behaviour. All systems with oligo(ethylene glycol) spacers were observed to adopt SmA phases, likely driven by the inherent segregation of oligo(ethylene glycol) units from alkyl group. A narrow range of gemini imidazolium-based LCs with alkyl spacers were capable of transitioning from crystalline to SmA thermotropic LC phases at different temperatures, driven by a shorter spacer paired with longer tails. For both sets of materials, tail and spacer lengths were also found to have a strong influence over the temperature range in which the thermotropic LC phase is stable. Anion type did not influence whether a thermotropic LC could be formed; however, systems with BF_4^- anions exhibited phase transitions at lower temperatures and smaller temperature windows of phase stability than analogues with two Br^- anions.

2. Experimental details

2.1 Materials

All chemicals were purchased from Sigma-Aldrich (Milwaukee, WI, USA). All manipulations were performed in air unless otherwise noted. Anhydrous THF was prepared by passing it over a column of activated Al_2O_3. 1,6-Dibromohexane and 1,8-dibromooctane were purified by passing the neat liquids through a plug of silica. 1,10-Dibromodecane was purified in a similar manner as a 50/50 (v/v) solution in *n*-hexane, followed by subsequent evaporation of *n*-hexane and crystallisation of the 1,10-dibromodecane. All other chemicals were used as received.

2.2 Synthesis of gemini imidazolium salts with long alkyl tails

Bisimidazole compounds **1–6** were synthesised in good yields from imidazole and the corresponding α,ω-dibromoalkane or oligo(ethylene glycol) α,ω-ditosylate according to procedures outlined in previous work from our group [16]. Subsequent reaction with 2.2 equivalents of a 1-bromoalkane produced the gemini imidazolium LC amphiphiles with bromide counterions **7a–16a**. Ion-exchange with a large excess of $NaBF_4$ in H_2O afforded the tetrafluoroborate salts **7b–16b** (Figure 3).

*2.2.1 Synthesis of 1,1′-(1,6-hexanediyl)bisimidazole (**1**)*

NaH (60 wt% dispersion in mineral oil, 14.70 g, 367.5 mmol) was introduced into a 1000 mL round-bottom flask equipped with a stir bar, reflux condenser and argon purge. Anhydrous THF (500 mL) was added and the mixture was stirred at ambient temperature. Imidazole (20.00 g, 293.8 mmol) was added slowly and gas bubbles began to evolve. When gas production had visibly stopped, the vessel was warmed to 40°C and further stirred for 30 min. After this time, 1,6-dibromohexane (32.28 g, 132.3 mmol) was added via syringe. The reaction was heated at reflux (65°C) under argon overnight. The reaction was allowed to cool to ambient temperature and the solids were filtered and washed with THF. The filtrate was reduced via rotary evaporation and extracted into MeOH (250 mL); an oily phase was observed to separate. Hexane was

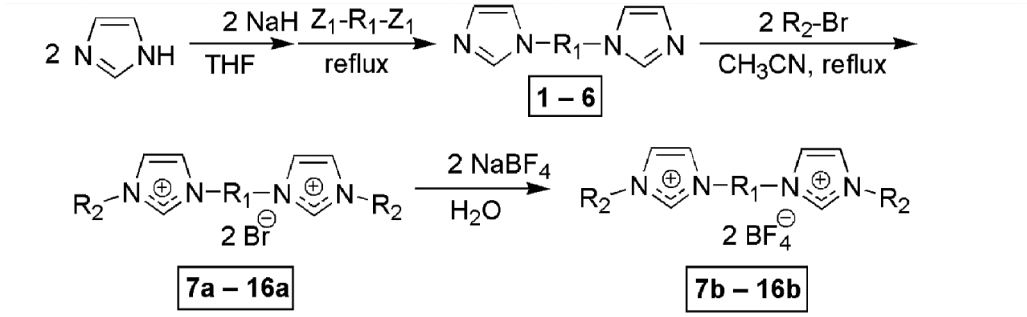

1: Z = Br, R_1 = -$(CH_2)_6$-
2: Z = Br, R_1 = -$(CH_2)_8$-
3: Z = Br, R_1 = -$(CH_2)_{10}$-
4: Z = TsO, R_1 = -$(CH_2)_2O(CH_2)_2$-
5: Z = TsO, R_1 = -$[(CH_2)_2O]_2(CH_2)_2$-
6: Z = TsO, R_1 = -$[(CH_2)_2O]_3(CH_2)_2$-
7: R_1 = -$(CH_2)_6$-, R_2 = -$(CH_2)_9CH_3$
8: R_1 = -$(CH_2)_6$-, R_2 = -$(CH_2)_{11}CH_3$
9: R_1 = -$(CH_2)_6$-, R_2 = -$(CH_2)_{13}CH_3$
10: R_1 = -$(CH_2)_8$-, R_2 = -$(CH_2)_{11}CH_3$
11: R_1 = -$(CH_2)_{10}$-, R_2 = -$(CH_2)_{11}CH_3$
12: R_1 = -$(CH_2)_2O(CH_2)_2$-, R_2 = -$(CH_2)_9CH_3$
13: R_1 = -$(CH_2)_2O(CH_2)_2$-, R_2 = -$(CH_2)_{11}CH_3$
14: R_1 = -$(CH_2)_2O(CH_2)_2$-, R_2 = -$(CH_2)_{13}CH_3$
15: R_1 = -$[(CH_2)_2O]_2(CH_2)_2$-, R_2 = -$(CH_2)_{11}CH_3$
16: R_1 = -$[(CH_2)_2O]_3(CH_2)_2$-, R_2 = -$(CH_2)_{11}CH_3$

Figure 3. Synthesis scheme for gemini imidazolium LC amphiphiles.

added to the MeOH phase until a separate hexanes phase was present on top. The MeOH phase was then further washed with hexanes (2 × 150 mL). The MeOH phase was reduced via rotary evaporation until a viscous liquid remained. The viscous liquid was dried under dynamic vacuum (<1 torr) overnight, producing a pale yellow (or orange) crystalline product. This solid was taken up in CH_2Cl_2 (250 mL) and the solution filtered through a plug of basic alumina. The alumina plug was washed with CH_2Cl_2 (2 × 125 mL) and the collected liquid phase reduced via rotary evaporation and dried under dynamic vacuum to provide **1** as an off-white solid. Yield = 27.20 g (94.2%). ^{1}H NMR (400 MHz, $CDCl_3$) δ 7.42 (s, 2H), 7.04 (s, 2H), 6.87 (d, J = 0.9, 2H), 3.89 (t, J = 7.0, 4H), 1.74 (m, 4H), 1.30 (m, 4H). HRMS: calculated as [M][H$^+$] = 219.1064; found = 219.1611.

*2.2.2 Synthesis of 1,1′-(1,8-octanediyl)bisimidazole (**2**)*

1,1′-(1,8-Octanediyl)bisimidazole (**2**) was produced from imidazole (20.00 g, 298.3 mmol) and 1,8-dibromooctane (36.00 g, 132.3 mmol) in a manner similar to that employed in the synthesis of **1**. Yield = 25.49g (78.2%). ^{1}H NMR (400 MHz, $CDCl_3$) δ 7.49 (d, J = 31.3, 2H), 7.03 (d, J = 19.8, 2H), 6.90 (d, J = 1.1, 2H), 3.92 (t, J = 7.1, 4H), 1.76 (dd, J = 7.1, 14.1, 4H), 1.28 (s, 8H). HRMS: calculated as [M][H$^+$] = 247.1917; found = 247.1908.

*2.2.3 Synthesis of 1,1′-(1,10-decanediyl)bisimidazole (**3**)*

1,1′-(1,10-Decanediyl)bisimidazole (**3**) was produced from imidazole (10.00 g, 146.9 mmol) and 1,10-dibromodecane (19.84 g, 66.11 mmol) in a manner similar to that employed in the synthesis of **1**. Yield = 17.53g (96.6%). ^{1}H NMR (400 MHz, $CDCl_3$) δ 7.44 (s, 2H), 7.02 (d, J = 10.4, 2H), 6.89 (t, J = 1.2, 2H), 3.90 (t, J = 7.1, 4H), 1.75 (dd, J = 7.0, 14.0, 4H), 1.29 (dd, J = 26.8, 31.9, 12H). HRMS: calculated as [M][H$^+$] = 275.2230; found = 275.2242.

*2.2.4 Synthesis of 1,1′-(oxydi-2,1-ethanediyl) bisimidazole (**4**)*

NaH (60 wt% in mineral oil, 11.00 g, 275.4 mmol) was added to a 1000 mL round-bottom flask equipped with a stir bar, reflux condenser and argon purge. Anhydrous THF (650 mL) was added and the mixture was stirred at ambient temperature. Imidazole (15.00 g, 220.3 mmol) was added slowly and gas bubbles were evolved. When gas production had visibly stopped, the vessel was warmed to 40°C and further stirred for 30 min. After this time, di(ethylene glycol) α,ω-ditosylate (41.09 g, 99.14 mmol) was added. The reaction was heated at reflux (65°C) under argon overnight. The reaction was allowed to cool to ambient temperature and the solids were filtered and washed with THF. The filtrate was reduced via rotary evaporation and extracted into MeOH (250 mL); an oily phase was observed to separate. Hexane was added to the MeOH phase until a separate hexane phase was present on top of the MeOH phase. The MeOH phase was then further washed with hexanes (2 × 150 mL). The MeOH phase was reduced via rotary evaporation until a viscous liquid remained. The viscous liquid was dried under dynamic vacuum (<1 torr) overnight, producing a red-brown oil. Yield = 18.30 g (89.5%). ^{1}H NMR (400 MHz, $CDCl_3$) δ 7.43 (s, 2H), 7.01 (m, 2H), 6.85 (t, J = 1.3, 2H), 4.04 (t, J = 5.1, 4H), 3.61 (m, 4H). HRMS: calculated as [M][H$^+$] = 207.1240; found = 207.1249.

*2.2.5 Synthesis of 1,1′-[1,2-ethanediylbis(oxy-2, 1-ethanediyl)]bisimidazole (**5**)*

1,1′-[1,2-Ethanediylbis(oxy-2,1-ethanediyl)]bisimidazole (**5**) was produced from imidazole (10.00 g, 146.9 mmol) and the α,ω-ditosylate of tri(ethylene glycol) (30.33 g, 66.11 mmol) in a manner similar to that employed in the synthesis of **4**. Yield = 14.19 g (85.7%). ^{1}H NMR (400 MHz, $CDCl_3$) δ 7.48 (s, 2H), 7.00 (s, 2H), 6.94 (m, 2H), 4.04 (t, J = 5.1, 4H), 3.61 (m, 4H), 3.49 (s, 4H). HRMS: calculated as [M][H$^+$] = 251.1502; found = 255.1511.

*2.2.6 Synthesis of 1,1′-[oxybis(2,1-ethanediyloxy-2,1-ethanediyl)]bisimidazole (**6**)*

1,1′-[Oxybis(2,1-ethanediyloxy-2,1-ethanediyl)]bisimidazole (**6**) was produced from imidazole (10.00 g, 146.9 mmol) and the α,ω-ditosylate of tetra(ethylene glycol) (33.23 g, 66.11 mmol) in a manner similar to that employed in the synthesis of **4**. Yield = 16.52 g (84.9%). ^{1}H NMR (400 MHz, $CDCl_3$) δ 7.49 (s, 2H), 6.96 (d, J = 16.3, 4H), 4.05 (t, J = 5.1, 4H), 3.68 (t, J = 5.1, 4H), 3.52 (s, 8H). HRMS: calculated as [M][H$^+$] = 295.1765; found = 295.1774.

*2.2.7 Synthesis of 1,1′-(1,6-hexanediyl)bis[3-decylimidazolium], bromide salt (**7a**)*

1,1′-(1,6-Hexanediyl)bisimidazole (**1**) (2.00 g, 9.16 mmol) was dissolved in CH_3CN (20 mL). 1-Bromodecane (4.46 g, 20.2 mmol) was added, and the reaction was heated at reflux (85°C) overnight. After this time, the reaction was allowed to cool and

was poured into anhydrous Et_2O (200 mL). White crystals formed immediately and the mixture was stored in a freezer at –10°C for 2 h. The crystals were then filtered, washed with Et_2O (100 mL), collected, and dried under dynamic vacuum to provide **7a** as a white powder. Yield = 5.20 g (85.9%). ^{1}H NMR (400 MHz, DMSO) δ 9.30 (s, 2H), 7.83 (s, 4H), 4.17 (t, J = 7.1, 8H), 1.80 (d, J = 6.9, 8H), 1.23 (s, 32H), 0.85 (t, J = 6.8, 6H). ^{13}C NMR (300 MHz, $CDCl_3$) δ 136.78, 123.56, 121.57, 50.21, 49.54, 31.94, 30.42, 29.55, 29.48, 29.34, 29.09, 26.39, 24.65, 22.77, 14.23. HRMS: calculated as $[A^{2+}][Br^-]$ = 579.3995; found = 579.3976.

*2.2.8 Synthesis of 1,1′-(1,6-hexanediyl)bis[3-decyl-imidazolium], tetrafluoroborate salt (**7b**)*

Compound **7a** (2.50 g, 3.78 mmol) was dissolved in warm deionised H_2O (100 mL). $NaBF_4$ (4.15 g, 37.8 mmol) was added and a precipitate formed immediately. The flask was then cooled in a refrigerator overnight. The precipitate was extracted into CH_2Cl_2 (100 mL) and the organic phase dried over $MgSO_4$. The solvent was reduced via rotary evaporation and the product dried under dynamic vacuum to provide **7b** as an off white, waxy powder. Yield = 2.38 g (93.4%). ^{1}H NMR (400 MHz, DMSO) δ 9.15 (s, 2H), 7.78 (dt, J = 1.8, 9.0, 4H), 4.15 (t, J = 7.2, 8H), 1.78 (m, 8H), 1.23 (s, 32H), 0.85 (t, J = 6.9, 6H). ^{13}C NMR (300 MHz, $CDCl_3$) δ 135.61, 123.07, 122.22, 50.22, 49.64, 32.00, 30.24, 29.62, 29.54, 29.41, 29.11, 26.39, 24.65, 22.81, 14.26. HRMS: calculated as $[A^{2+}][BF_4^-]$ = 587.4847; found = 587.4855.

*2.2.9 Synthesis of 1,1′-(1,6-hexanediyl)bis[3-dodecyl-imidazolium], bromide salt (**8a**)*

Compound **8a** was produced from **1** (2.00 g, 9.16 mmol) and 1-bromododecane (5.02 g, 20.2 mmol) in a manner similar to that employed in the synthesis of **7a**. Yield = 5.83 g (88.8%). ^{1}H NMR (400 MHz, DMSO) δ 9.25 (s, 2H), 7.81 (t, J = 1.4, 4H), 4.16 (t, J = 7.2, 8H), 1.79 (d, J = 6.8, 8H), 1.23 (s, 40H), 0.85 (t, J = 6.9, 6H). ^{13}C NMR (300 MHz, $CDCl_3$) δ 136.88, 123.55, 121.56, 50.23, 49.56, 32.01, 30.43, 29.71, 29.61, 29.55, 29.50, 29.44, 29.11, 26.41, 24.66, 22.80, 14.25. HRMS: calculated as $[A^{2+}][Br^-]$ = 635.4621; found = 635.4631.

*2.2.10 Synthesis of 1,1′-(1,6-hexanediyl)bis[3-dodecyl-imidazolium], tetrafluoroborate salt (**8b**)*

Compound **8b** was produced from **8a** (3.00 g, 4.19 mmol) and $NaBF_4$ (4.60 g, 41.9 mmol) in a manner similar to that employed in the synthesis of **7b**. Yield = 2.62 g (85.7%). ^{1}H NMR (400 MHz, DMSO) δ 9.15 (s, 2H), 7.79 (dt, J = 1.8, 9.5, 4H), 4.14 (t, J = 7.2, 8H), 1.79 (dd, J = 7.0, 13.8, 8H), 1.24 (d, J = 8.3, 40H), 0.85 (t, J = 6.9, 6H). ^{13}C NMR (300 MHz, $CDCl_3$) δ 135.69, 123.12, 122.16, 50.26, 49.67, 32.08, 30.28, 29.80, 29.71, 29.59, 29.52, 29.39, 29.15, 26.44, 24.65, 22.86, 14.30. HRMS: calculated as $[A^{2+}][BF_4^-]$ = 643.5474; found = 643.5465.

*2.2.11 Synthesis of 1,1′-(1,6-hexanediyl)bis[3-tetradecyl-imidazolium], bromide salt (**9a**)*

Compound **9a** was produced from **1** (2.00 g, 9.16 mmol) and 1-bromotetradecane (5.59 g, 20.2 mmol) in a manner similar to that employed in the synthesis of **7a**. Yield = 5.97 g (84.3%). ^{1}H NMR (400 MHz, DMSO) δ 9.27 (s, 2H), 7.82 (d, J = 1.6, 4H), 4.16 (t, J = 6.9, 8H), 1.78 (s, 8H), 1.23 (s, 48H), 0.85 (t, J = 6.9, 6H). ^{13}C NMR (300 MHz, $CDCl_3$) δ 136.76, 123.51, 121.60, 50.17, 49.51, 31.98, 30.39, 29.74, 29.71, 29.67, 29.58, 29.52, 29.47, 29.42, 29.07, 26.36, 24.63, 22.75, 14.20. HRMS: calculated as $[A^{2+}][Br^-]$ = 691.5247; found = 691.5266.

*2.2.12 Synthesis of 1,1′-(1,6-hexanediyl)bis[3-tetradecyl-imidazolium], tetrafluoroborate salt (**9b**)*

Compound **9b** was produced from **9a** (3.00 g, 3.88 mmol) and $NaBF_4$ (4.26 g, 38.8 mmol) in a manner similar to that employed in the synthesis of **7b**. Yield = 2.35 g (77.1%). ^{1}H NMR (400 MHz, DMSO) δ 9.16 (s, 2H), 7.79 (dt, J = 1.8, 9.3, 4H), 4.14 (t, J = 7.2, 8H), 1.78 (m, 8H), 1.23 (s, 48H), 0.85 (t, J = 6.9, 6H). ^{13}C NMR (300 MHz, $CDCl_3$) δ 135.71, 123.13, 122.13, 50.27, 49.68, 32.11, 30.29, 29.89, 29.86, 29.85, 29.82, 29.74, 29.61, 29.55, 29.38, 29.17, 26.45, 24.64, 22.88, 14.37. HRMS: calculated as $[A^{2+}][BF_4^-]$ = 699.6100; found = 699.6117.

*2.2.13 Synthesis of 1,1′-(1,8-octanediyl)bis[3-dodecyl-imidazolium], bromide salt (**10a**)*

Compound **10a** was produced from **2** (3.00 g, 12.2 mmol) and 1-bromododecane (6.69 g, 26.8 mmol) in a manner similar to that employed in the synthesis of **7a.** Yield = 7.79 g (85.7%). ^{1}H NMR (400 MHz, DMSO) δ 9.34 (s, 2H), 7.84 (p, J = 2.0, 4H), 4.17 (t, J = 7.1, 8H), 1.78 (m, 8H), 1.24 (d, J = 15.4, 44H), 0.84 (t, J = 6.9, 6H). ^{13}C NMR (300 MHz, $CDCl_3$) δ 136.64, 123.03, 121.86, 49.98, 49.67, 31.83, 30.33, 29.66, 29.53, 29.45, 29.34, 29.27, 28.96, 27.66, 26.22, 25.27, 22.62, 14.08. HRMS: calculated as $[A^{2+}][Br^-]$ = 663.4934; found = 663.4944.

*2.2.14 Synthesis of 1,1′-(1,8-octanediyl)bis [3-dodecyl-imidazolium], tetrafluoroborate salt (**10b**)*

Compound **10b** was produced from **10a** (3.00 g, 4.03 mmol) and $NaBF_4$ (4.42 g, 40.3 mmol) in a manner similar to that employed in the synthesis of **7b**. Yield = 2.12 g (69.2%). ^{1}H NMR (400 MHz, DMSO) δ 9.17 (s, 2H), 7.79 (dt, J = 1.8, 6.4, 4H), 4.14 (td, J = 1.9, 7.2, 8H), 1.78 (dd, J = 6.6, 14.0, 8H), 1.25 (d, J = 15.3, 44H), 0.85 (t, J = 6.8, 6H). ^{13}C NMR (300 MHz, $CDCl_3$) δ 135.74, 122.96, 122.26, 50.27, 50.04, 32.09, 30.33, 29.81, 29.72, 29.60, 29.53, 29.17, 27.74, 26.43, 25.32, 22.87, 14.31. HRMS: calculated as $[A^{2+}][BF_4^-]$ = 671.5787; found = 671.5809.

*2.2.15 Synthesis of 1,1′-(1,10-decanediyl)bis [3-dodecyl-imidazolium], bromide salt (**11a**)*

Compound **11a** was produced from **3** (3.00 g, 10.9 mmol) and 1-bromododecane (5.98 g, 24.0 mmol) in a manner similar to that employed in the synthesis of **7a**. Yield = 6.13 g (72.8%). ^{1}H NMR (400 MHz, DMSO) δ 9.27 (s, 2H), 7.82 (s, 4H), 4.16 (t, J = 7.0, 8H), 1.78 (m, 8H), 1.22 (s, 48H), 0.85 (t, J = 6.6, 6H). ^{13}C NMR (300 MHz, $CDCl_3$) δ 137.00, 122.88, 122.04, 50.16, 49.95, 32.01, 30.50, 30.09, 29.71, 29.62, 29.52, 29.44, 29.14, 28.60, 28.27, 26.39, 25.77, 22.79, 14.25. HRMS: calculated as $[A^{2+}][Br^-]$ = 691.5247, found = 691.5240.

*2.2.16 Synthesis of 1,1′-(1,10-decanediyl)bis [3-dodecyl-imidazolium], tetrafluoroborate salt (**11b**)*

Compound **11b** was produced from **11a** (3.00 g, 3.88 mmol) and $NaBF_4$ (4.26 g, 38.8 mmol) in a manner similar to that employed in the synthesis of **7b**. Yield = 2.48 g (81.2%). ^{1}H NMR (400 MHz, DMSO) δ 9.17 (s, 2H), 7.79 (m, 4H), 4.15 (dd, J = 4.1, 9.9, 8H), 1.78 (dd, J = 6.8, 13.6, 8H), 1.24 (d, J = 14.6, 48H), 0.85 (t, J = 6.8, 6H). ^{13}C NMR (300 MHz, $CDCl_3$) δ 135.67, 122.87, 122.38, 50.22, 50.08, 32.06, 30.32, 29.91, 29.78, 29.77, 29.69, 29.57, 29.50, 29.14, 28.59, 28.29, 26.38, 25.74, 22.84, 14.28. HRMS: calculated as $[A^{2+}][BF_4^-]$ = 699.6100; found = 699.6099.

*2.2.17 Synthesis of 1,1′-(oxydi-2,1-ethanediyl)bis [3-decyl-imidazolium], bromide salt (**12a**)*

Compound **12a** was produced from **4** (2.00 g, 9.70 mmol) and 1-bromodecane (4.72 g, 21.3 mmol) in a manner similar to that employed in the synthesis of **7a**. Yield = 4.83 g (76.8%). ^{1}H NMR (400 MHz, DMSO) δ 9.34 (s, 2H), 7.79 (dt, J = 1.8, 26.6, 4H), 4.38 (m, 4H), 4.20 (t, J = 7.3, 4H), 3.79 (m, 4H), 1.79 (dd, J = 7.2, 14.1, 4H), 1.23 (s, 28H), 0.85 (t, J = 6.9, 6H). ^{13}C NMR (300 MHz, $CDCl_3$) 137.20, 124.13, 121.34, 69.35, 50.21, 49.80, 31.98, 30.57, 29.61, 29.55, 29.39, 29.19, 26.43, 22.80, 14.26. HRMS: calculated as $[A^{2+}][Br^-]$ = 567.3632; found = 567.3635.

*2.2.18 Synthesis of 1,1′-(oxydi-2,1-ethanediyl)bis [3-decyl-imidazolium], tetrafluoroborate salt (**12b**)*

Compound **12b** was produced from **12a** (2.00 g, 3.08 mmol) and $NaBF_4$ (3.38 g, 30.8 mmol) in a manner similar to that employed in the synthesis of **7b**. Yield = 1.15 g (56.5%) of a viscous yellow honey-like oil were collected from the flask. The total yield is greater. ^{1}H NMR (400 MHz, DMSO) δ 9.05 (s, 2H), 7.70 (dt, J = 1.7, 39.5, 4H), 4.32 (m, 4H), 4.13 (t, J = 7.3, 4H), 3.75 (m, 4H), 1.77 (dd, J = 7.2, 14.2, 4H), 1.22 (s, 28H), 0.84 (t, J = 6.8, 6H). ^{13}C NMR (300 MHz, $CDCl_3$) δ 136.17, 123.54, 121.95, 68.81, 50.17, 49.72, 32.01, 30.27, 29.66, 29.59, 29.43, 29.17, 26.42, 22.81, 14.25. HRMS: calculated as $[A^{2+}][BF_4^-]$ = 575.4483; found = 575.4506.

*2.2.19 Synthesis of 1,1′-(oxydi-2,1-ethanediyl)bis [3-dodecyl-imidazolium], bromide salt (**13a**)*

Compound **13a** was produced from **4** (5.00 g, 24.2 mmol) and 1-bromododecane (13.27 g, 53.24 mmol) in a manner similar to that employed in the synthesis of **7a**. Yield = 14.71 g (86.4%). ^{1}H NMR (400 MHz, DMSO) δ 9.29 (s, 2H), 7.76 (dt, J = 1.7, 28.0, 4H), 4.36 (m, 4H), 4.17 (t, J = 7.3, 4H), 3.77 (m, 4H), 1.77 (dd, J = 7.2, 14.2, 4H), 1.21 (s, 36H), 0.83 (t, J = 6.8, 6H). ^{13}C NMR (300 MHz, $CDCl_3$) δ 137.39, 124.09, 121.33, 69.31, 50.19, 49.78, 32.03, 30.55, 29.73, 29.65, 29.55, 29.46, 29.18, 29.42, 22.81, 14.26. HRMS: calculated as $[A^{2+}][Br^-]$ = 623.4258; found = 623.4250.

*2.2.20 Synthesis of 1,1′-(oxydi-2,1-ethanediyl)bis [3-dodecyl-imidazolium], tetrafluoroborate salt (**13b**)*

Compound **13b** was produced from **13a** (5.00 g, 7.10 mmol) and $NaBF_4$ (7.80 g, 71.0 mmol) in a manner similar to that employed in the synthesis of **7b**. Yield = 4.20 g (82.3%). ^{1}H NMR (400 MHz, DMSO) δ 9.06 (s, 2H), 7.72 (dt, J = 1.8, 40.1, 4H), 4.34 (m, 4H), 4.15 (t, J = 7.3, 4H), 3.77 (m, 4H), 1.78 (dd, J = 7.2, 14.1, 4H), 1.24 (s, 36H), 0.85 (t, J = 6.8, 6H). ^{13}C NMR (300 MHz, $CDCl_3$) δ 136.42, 123.58, 121.93, 68.83, 50.21, 49.78, 32.10, 30.33, 29.83, 29.82, 29.76, 29.65, 29.54, 29.23, 26.47, 22.87, 14.30. HRMS: calculated as $[A^{2+}][BF_4^-]$ = 631.5110; found = 631.5116.

*2.2.21 Synthesis of 1,1′-(oxydi-2,1-ethanediyl)bis [3-tetradecyl-imidazolium], bromide salt (**14a**)*

Compound **14a** was produced from **4** (2.00 g, 9.70 mmol) and 1-bromotetradecane (5.92 g, 21.3 mmol) in a manner similar to that employed in the synthesis of **7a**. Yield = 6.09 g (82.5%). ^{1}H NMR (400 MHz, DMSO) δ 9.30 (s, 2H), 7.78 (dt, J = 1.8, 28.8, 4H), 4.38 (m, 4H), 4.19 (t, J = 7.3, 4H), 3.79 (m, 4H), 1.79 (dd, J = 7.2, 14.0, 4H), 1.23 (s, 44H), 0.85 (t, J = 6.8, 6H). ^{13}C NMR (300 MHz, $CDCl_3$) δ 137.25, 124.02, 121.39, 69.25, 50.15, 49.74, 32.00, 30.51, 29.77, 29.74, 29.71, 29.63, 29.52, 29.44, 29.16, 26.39, 22.77, 14.22. HRMS: calculated as $[A^{2+}][Br^-]$ = 679.4884; found = 679.4889.

*2.2.22 Synthesis of 1,1′-(oxydi-2,1-ethanediyl)bis [3-tetradecyl-imidazolium], tetrafluoroborate salt (**14b**)*

Compound **14b** was produced from **14a** (3.00 g, 3.94 mmol) and $NaBF_4$ (4.33 g, 39.4 mmol) in a manner similar to that employed in the synthesis of **7b**. Yield = 2.85 g (93.4%). ^{1}H NMR (400 MHz, DMSO) δ 9.07 (s, 2H), 7.72 (dt, J = 1.8, 40.7, 4H), 4.34 (m, 4H), 4.14 (t, J = 7.3, 4H), 3.77 (m, 4H), 1.77 (m, 4H), 1.24 (s, 44H), 0.85 (t, J = 6.9, 6H). ^{13}C NMR (300 MHz, $CDCl_3$) δ 136.25, 123.57, 121.90, 68.82, 50.20, 49.76, 32.10, 30.32, 29.89, 29.88, 29.85, 29.78, 29.66, 29.55, 29.23, 26,47, 22.87, 14.30. HRMS: calculated as $[A^{2+}][BF_4^-]$ = 687.5736; found = 687.5742.

*2.2.23 Synthesis of 1,1′-[1,2-ethanediylbis(oxy-2, 1-ethanediyl)]bis[1-dodecyl-imidazolium], bromide salt (**15a**)*

Compound **15a** was produced from **5** (5.00 g, 20.0 mmol) and 1-bromododecane (10.97 g, 44.00 mmol) in a manner similar to that employed in the synthesis of **7a**. Yield = 13.59 g (90.8%). ^{1}H NMR (400 MHz, DMSO) δ 9.24 (s, 2H), 7.80 (dt, J = 1.7, 27.1, 4H), 4.35 (t, J = 4.9, 4H), 4.19 (t, J = 7.2, 4H), 3.75 (m, 4H), 3.53 (s, 4H), 1.77 (m, 4H), 1.23 (s, 36H), 0.85 (t, J = 6.8, 6H). ^{13}C NMR (300 MHz, $CDCl_3$) δ 136.93, 123.68, 121.96, 70.74, 69.20, 50.20, 49.93, 31.97, 30.47, 29.68, 29.60, 29.51, 29.40, 29.13, 26.37, 22.75, 14.21. HRMS: calculated as $[A^{2+}][Br^-]$ = 667.4520; found = 667.4527.

*2.2.24 Synthesis of 1,1′-[1,2-ethanediylbis(oxy-2, 1-ethanediyl)]bis[1-dodecyl-imidazolium], tetrafluoroborate salt (**15b**)*

Compound **15b** was produced from **15a** (5.00 g, 6.68 mmol) and $NaBF_4$ (7.33 g, 66.8 mmol) in a manner similar to that employed in the synthesis of **7b**. Yield = 3.65 g (71.7%) as a hard white wax. ^{1}H NMR (400 MHz, DMSO) δ 9.11 (s, 2H), 7.75 (dt, J = 1.7, 29.3, 4H), 4.32 (t, J = 4.9, 4H), 4.16 (t, J = 7.2, 4H), 3.74 (m, 4H), 3.52 (s, 4H), 1.78 (dd, J = 7.2, 14.3, 4H), 1.25 (d, J = 14.1, 36H), 0.85 (t, J = 6.8, 6H). ^{13}C NMR (300 MHz, $CDCl_3$) δ 136.08, 123.56, 122.08, 70.65, 68.91, 50.22, 50.03, 32.08, 30.30, 29.81, 29.80, 29.73, 29.62, 29.52, 29.19, 26.42, 22.85, 14.29. HRMS: calculated as $[A^{2+}][BF_4^-]$ = 675.5372; found = 675.5361.

*2.2.25 Synthesis of 1,1′-[oxybis(2,1-ethanediyloxy-2, 1-ethanediyl]bis[1-dodecyl-imidazolium], bromide salt (**16a**)*

Compound **16a** was produced from **6** (5.00 g, 17.0 mmol) and 1-bromododecane (9.32 g, 37.4 mmol) in a manner similar to that employed in the synthesis of **7a**. Yield = 10.58 g (78.5 %). ^{1}H NMR (400 MHz, DMSO) δ 9.31 (d, J = 17.8, 2H), 7.85 (dt, J = 1.7, 21.2, 4H), 4.38 (t, J = 4.9, 4H), 4.20 (t, J = 7.2, 4H), 3.78 (m, 4H), 3.49 (m, 8H), 1.78 (dd, J = 7.1, 14.2, 4H), 1.22 (s, 36H), 0.84 (t, J = 6.8, 6H). ^{13}C NMR (300 MHz, $CDCl_3$) δ 136.64, 123.39, 121.82, 70.39, 70.32, 68.95, 49.97, 49.54, 31.78, 30.26, 29.48, 29.41, 29.31, 29.21, 28.93, 26.17, 22.56, 14.02. HRMS: calculated as $[A^{2+}][Br^-]$ = 711.4782; found = 711.4801.

*2.2.26 Synthesis of 1,1′-[oxybis(2,1-ethanediyloxy-2, 1-ethanediyl]bis[1-dodecyl-imidazolium], bromide salt (**16b**)*

Compound **16b** was produced from **16a** (3.00 g, 3.78 mmol) and $NaBF_4$ (4.15 g, 37.8 mmol) in a manner similar to that employed in the synthesis of **7b**. Yield = 1.51 g (49.5%) of a viscous yellow honey-like oil was collected from the flask. The total yield is greater. ^{1}H NMR (400 MHz, DMSO) δ 9.11 (s, 2H), 7.75 (m, 4H), 4.33 (m, 4H), 4.16 (t, J = 7.2, 4H), 3.76 (m, 4H), 3.49 (m, 8H), 1.77 (m, 4H), 1.23 (s, 36H), 0.85 (t, J = 6.8, 6H). ^{13}C NMR (300 MHz, $CDCl_3$) δ 136.07, 123.54, 122.05, 70.55, 70.42, 68.88, 50.19, 49.80, 32.06, 30.28, 29.80, 29.78, 29.72, 29.60, 29.50, 29.18, 26.40, 22.84, 14.28. HRMS: calculated as $[A^{2+}][BF_4^-]$ = 719.5634; found = 719.5624.

2.3 Polarised light microscopy (PLM) analysis

The temperature range of each thermotropic LC phase was determined using variable temperature polarised light microscopy (PLM). PLM studies were performed using a Leica DMRXP polarising light microscope equipped with a Linkam LTS 350 thermal

stage, Linkam CI 94 temperature controller, and a Q-Imaging MicroPublisher 3.3 RTV digital camera. Linkam Linksys32 software was used to automate temperature profiles and for image capturing. Specimens for PLM were prepared by pressing samples between a microscope slide and microscope coverslip. The sample was placed on the PLM thermal stage and annealed past its isotropic temperature or up to 250°C if no isotropic phase was reached. The sample was slowly cooled and allowed to come back to its room temperature phase. The sample was then heated to past its isotropic temperature or up to 250°C at a rate of 5°C/min with image capture at every 1.25°C and continuous recording of the light intensity. Changes in optical texture and light intensity were used to determine changes in the phase of the mixture.

2.4 Powder X-ray diffraction (XRD) analysis

Powder XRD profiles were obtained using an Inel CPS 120 X-ray diffraction system equipped with a Cu-K_α source and a custom-built rotating sample pan heater system. All XRD spectra were calibrated against a silver behenate line spacing diffraction standard (d_{100} = 58 Å) [41]. For crystalline samples, XRD profiles were collected for 15 min. XRD profiles of thermotropic LC phases and isotropic samples were obtained by heating the compound above the range in which its crystalline phase is stable (if above ambient temperature), and collecting data for 5 min.

3. Results and discussion

Given the large number of symmetric gemini imidazolium ionic amphiphiles possible (Figure 2(b)), it should be noted that this study is by no means intended to be comprehensive in nature. However, we feel that the parameters examined in this initial work with these 20 symmetric gemini imidazolium amphiphiles provide insight to the effects and trends that various spacer-tail-anion combinations can have on the thermotropic LC behaviour of this class of ionic molecules.

Table 1 presents the thermotropic LC phase behaviour of the 20 gemini imidazolium amphiphiles synthesised. The identities of the thermotropic LC phases observed for these compounds were determined using PLM optical texture analysis and powder XRD analysis at various temperatures.

XRD profiles (2θ = 0.5–40°) for each of the gemini imidazolium compounds in their respective crystalline, SmA, and isotropic states can be found in

Table 1. Summary of thermotropic LC phase behaviours of a series of 20 symmetric gemini imidazolium salts.

Compound	MW	R_1	R_2	X	Phase Transition Behaviour (°C)					*d*(Å)
7a	660.65	C_6	C_{10}	Br	Cr	72	Iso			
7b	674.45	C_6	C_{10}	BF_4	Cr	70	Iso			
8a	716.76	C_6	C_{12}	Br	Cr	75	SmA	150	Iso	30.6
8b	730.56	C_6	C_{12}	BF_4	Cr	31	SmA	69	Iso	30.4
9a	772.87	C_6	C_{14}	Br	Cr	89	SmA	>200	Iso	36.4
9b	786.67	C_6	C_{14}	BF_4	Cr	88	SmA	173	Iso	32.9
10a	744.81	C_8	C_{12}	Br	Cr	114	Iso			
10b	758.61	C_8	C_{12}	BF_4	Cr	70	Iso			
11a	772.87	C_{10}	C_{12}	Br	Cr	100	Iso			
11b	786.67	C_{10}	C_{12}	BF_4	Cr	55	Iso			
12a	648.60	PEG_1	C_{10}	Br	Cr	<22	SmA	127	Iso	28.7
12b	662.40	PEG_1	C_{10}	BF_4	Cr	<22	SmA	27	Iso	29.0
13a	704.71	PEG_1	C_{12}	Br	Cr	104	SmA	>200	Iso	33.5
13b	718.51	PEG_1	C_{12}	BF_4	Cr	<22	SmA	148	Iso	32.4
14a	760.81	PEG_1	C_{14}	Br	Cr	98	SmA	>200	Iso	37.6
14b	774.61	PEG_1	C_{14}	BF_4	Cr	42	SmA	>200	Iso	35.5
15a	748.76	PEG_2	C_{12}	Br	Cr	73	SmA	93	Iso	30.7
15b	762.56	PEG_2	C_{12}	BF_4	Cr	29	SmA	50	Iso	30.2
16a	792.81	PEG_3	C_{12}	Br	Cr[a]	<22	SmA	30	Iso	30.2
16b	806.61	PEG_3	C_{12}	BF_4	Cr[a]	<22	SmA	37	Iso	29.4

Notes: PEG_1 = -$(CH_2)_2O(CH_2)_2$-.
PEG_2 = -$[(CH_2)_2O]_2(CH_2)_2$-.
PEG_3 = -$[(CH_2)_2O]_3(CH_2)_2$-.
Cr = crystalline phase.
d (Å) = *d*-spacing of first peak in XRD profile of LC phase.
Iso = isotropic liquid phase.
[a]After product isolation, a slow transition to SmA occurred from what was initially an isotropic state at room temperature (22 ± 2°C) over several months.

the supplementary material which is available via the multimedia link on the online article webpage.

As can be seen in Table 1, more than half of the gemini imidazolium systems with alkyl spacers exhibit no thermotropic LC behaviour. They transition from ordered, crystalline salts to molten salts without an intermediate ordered LC state. The gemini imidazolium salts with *n*-hexyl spacers and *n*-decyl tails (**7a,b**) as well as those with *n*-octyl and *n*-decyl spacers (**10a,b** and **11a,b**) exhibit no thermotropic LC properties in their neat states. Only certain systems with *n*-hexyl spacer and *n*-dodecyl or *n*-tetradecyl tails (**8a,b** and **9a,b**) are able to adopt thermotropic LC phases. When hydrocarbon groups are exclusively used to constitute the non-ionic components of the gemini imidazolium salts, there appears to be a spacer length-to-tail length balance that must be satisfied in order to promote thermotropic LC phase formation. Too short a pendant alkyl tail, too little hydrocarbon bulk in the tails or too much length in the ionic headgroup spacer produces materials that melt into gemini ILs without forming any intermediate ordered LC phases. In addition, the anion type (Br^- or BF_4^-) appears to have no effect on whether or not a thermotropic LC phase can be formed in the alkyl or oligo(ethylene glycol)-bridged molecules.

Figure 4 shows two of the more visually distinctive PLM optical textures exhibited by the family of gemini imidazolium amphiphiles synthesised in this study. These optical texture images are associated with the crystalline phases of the alkyl-bridged gemini imidazolium salts. Figure 5 shows the XRD profiles of the same gemini imidazolium salts in these crystalline phases.

Figures 4 and 5 are presented largely for reference purposes and to illustrate the results of analysing crystalline gemini imidazolium salts, and for comparison with the data obtained from thermotropic LC phases in analogous systems. No attempts were made

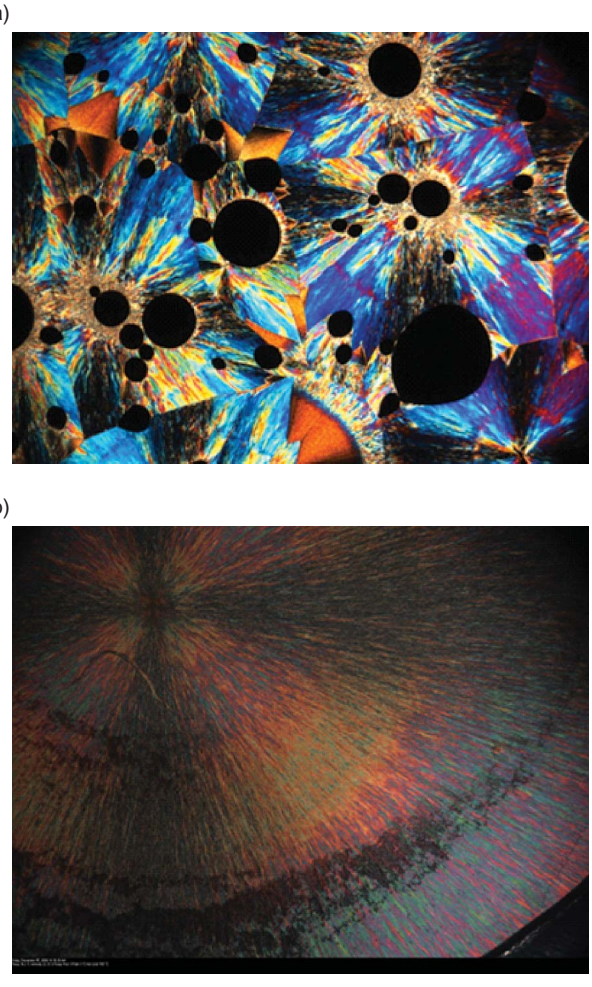

Figure 4. PLM images (250 × magnification) of crystalline phases of gemini imidazolium amphiphiles with *n*-dodecyl tails: (a) *n*-octyl spacer (**10b**); and (b) *n*-decyl spacer (**11b**).

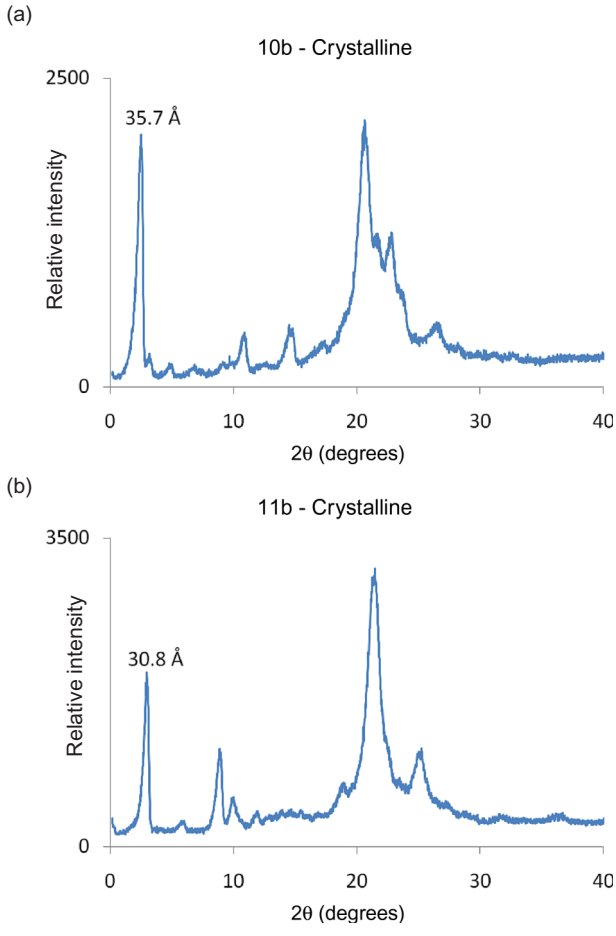

Figure 5. Powder XRD profiles of crystalline phases of gemini imidazolium amphiphiles with *n*-dodecyl tails: (a) octyl spacer (**10b**); (b) decyl spacer (**11b**).

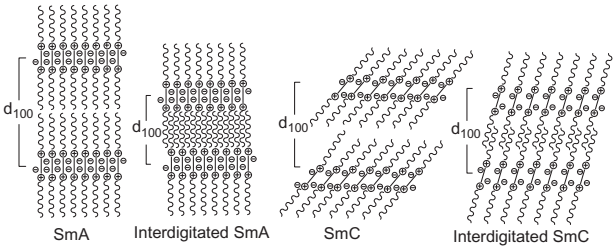

Figure 6. Representation of amphiphilic gemini cations in a thermotropic SmA phase with little or no alkyl tail interdigitation, a SmA phase with alkyl tail interdigitation, a SmC phase with little or no alkyl tail interdigitation, and a SmC phase with some tail interdigitation.

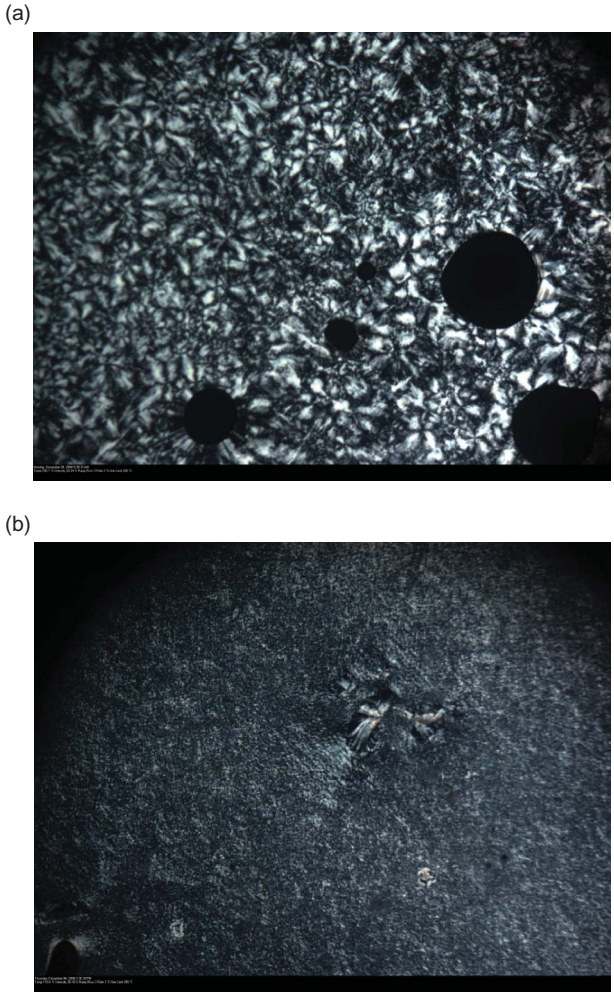

Figure 7. Representative PLM images (250 × magnification) of thermotropic LC phases of gemini imidazolium salts with *n*-hexyl spacers: (a) *n*-dodecyl tails (**8a**) at 100°C; and (b) *n*-tetradecyl tails (**9b**) at 110°C.

to resolve a crystal structure for these or any other crystalline phase found in the gemini imidazolium systems studied.

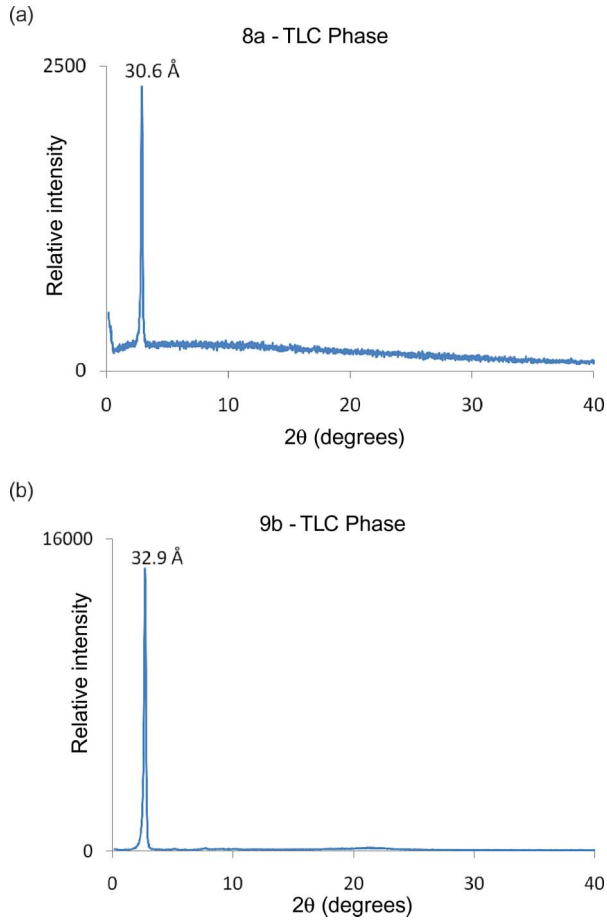

Figure 8. XRD profiles of thermotropic LC phases observed in gemini imidazolium amphiphiles with an *n*-hexyl spacer: (a) *n*-dodecyl tails (**8a**); and (b) *n*-tetradecyl tails (**9b**).

Four alkyl-bridged gemini imidazolium systems (**8a,b** and **9a,b**) displayed thermotropic SmA phases at elevated temperatures as determined by XRD analysis and visually confirmed via PLM image analysis [42]. Typically, lamellar Sm phases are characterised by focal conic type PLM optical textures, and XRD profiles with *d*-spacing peaks (Å) that proceed in the ratio 1:1/2:1/3 . . . [43]. In these systems, the primary *d*-spacing peak (d_{100}) represents the average layer distance in the lamellar phase structure [43]. If the observed primary *d*-spacing value is approximately the calculated extended length of the amphiphilic molecule, then the molecules are most likely arranged in a non-tilted lamellar pattern (i.e. a SmA phase) (Figure 6(a)) [43]. However, if the observed lamellar *d*-spacing value is substantially smaller than the extended length of the amphiphilic molecule, then either a tail-interdigitated, non-tilted SmA phase (Figure 6(b)), or a tilted lamellar phase (i.e. a SmC phase) without or with some tail interdigitation is present (Figure 6(c) and 6(d)) [42, 43].

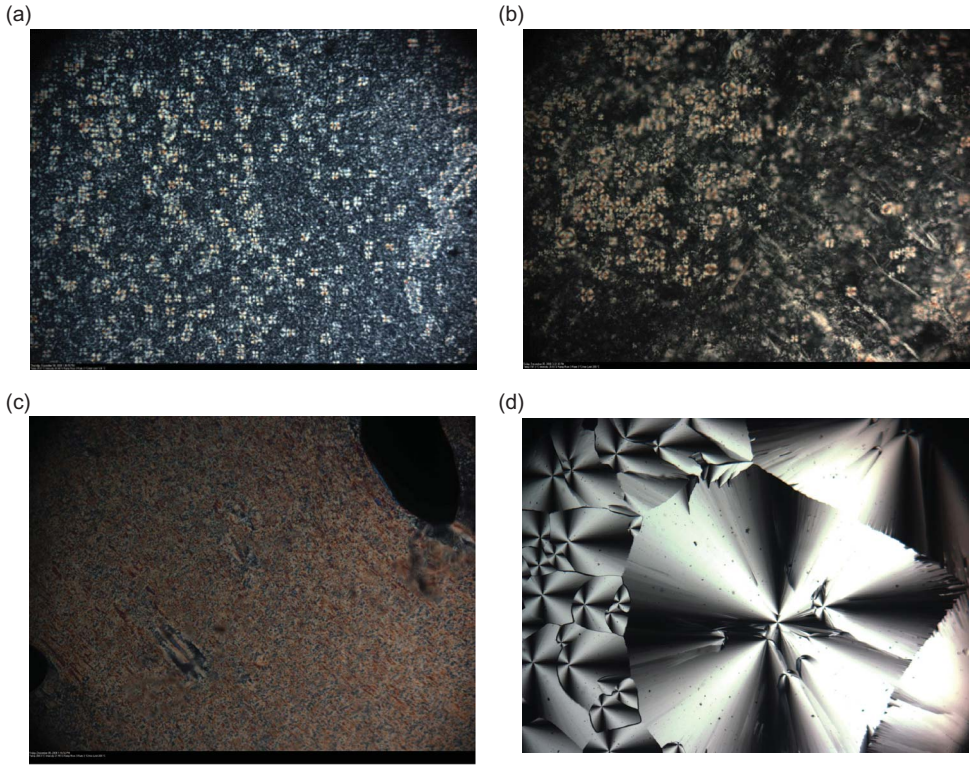

Figure 9. Representative PLM images (250 × magnification) of thermotropic LC phases of gemini imidazolium amphiphiles with oligo(ethylene glycol) spacers: (a) **12a** at 25°C; (b) **13a** at 200°C; (c) **14b** at 200°C; and (d) **15b** at 30°C (colour version online).

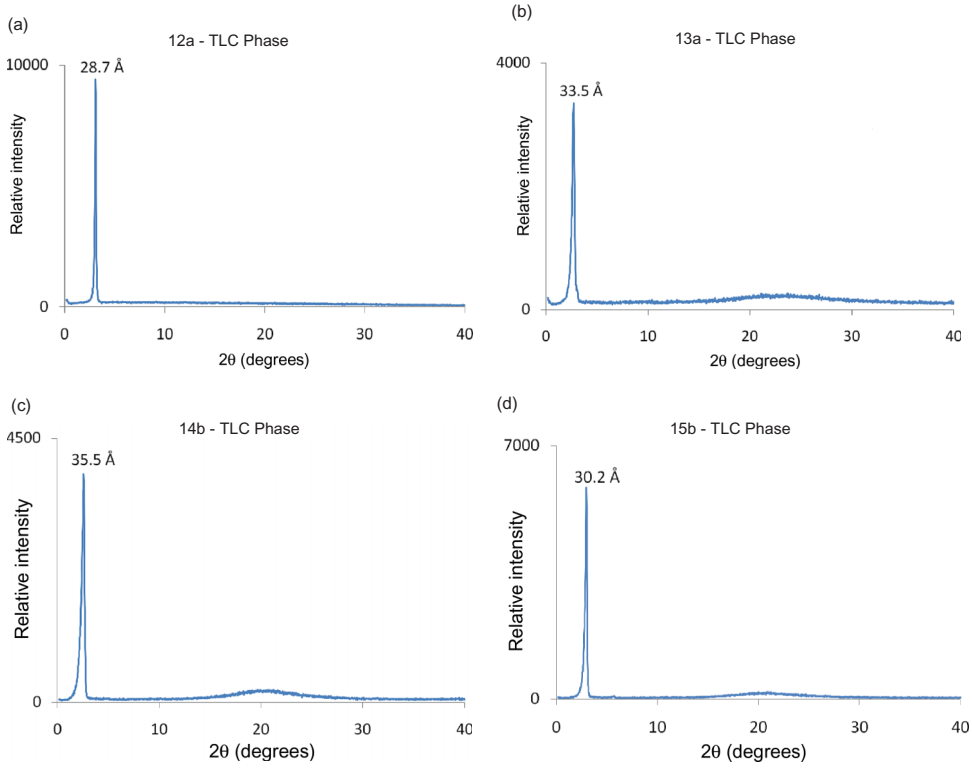

Figure 10. Powder XRD profiles of selected gemini imidazolium amphiphiles with oligo(ethylene glycol) spacers: (a) **12a**; (b) **13a**; (c) **14b**; and (d) **15b** (colour version online).

Given the symmetric nature of the gemini imidazolium amphiphiles studied [14, 39] and the reported LC behaviour of similar ammonium and phosphonium systems, a non-tilted SmA phase with alkyl tail interdigitation (Figure 6(b)) is expected to be predominant [4, 9–11].

Using a simple molecular modelling approach [42], the fully extended lengths of the gemini imidazolium compounds were found to be in the range of 40–55 Å. Each of the *d*-spacings presented in Table 1, as determined by XRD analysis, are less than those of fully extended lengths. This suggests that either a SmA phase with alkyl tail interdigitation between layers is present, or a tilted SmC phase with or without some tail interdigitation. The presence of focal conic PLM optical textures in each of these systems suggests that SmA phases with tail interdigitation are most likely formed, since these types of textures are characteristic of SmA phases [42]. Example XRD and optical textures for selected gemini imidazolium LCs follow.

Figures 7 and 8 show images obtained via PLM analysis and XRD profiles for the LC phases exhibited by compounds **8a** and **9b**.

It appears that a shorter spacer unit between the imidazolium headgroups is necessary to achieve thermotropic LC behaviour in these systems. Compounds **9a** and **11a** (also **9b** and **11b**) are structural isomers, with **9a** having a shorter spacer and longer tails than **11a**. The shorter spacer length places the cations and anions closer in proximity within the central region of these molecules. We speculate these more localised ionic interactions may afford central cores in these calamitic molecules that are more chemically different and possibly less conformationally mobile than the flexible, hydrophobic, long alkyl tails at the ends. These effects would enhance local phase separation on multiple levels (i.e. ionic/hydrophilic vs. hydrophobic, and hard vs. soft) that would help thermotropic, layered (i.e. Sm) LC phase formation.

Interestingly, all of the gemini imidazolium salts synthesised with oligo(ethylene glycol) spacers exhibited thermotropic LC behaviour. This is in sharp contrast to analogues with only alkyl spacers. The presence of a polar linkage in the spacer between the imidazolium rings apparently adds another dimension and additional driving force for LC self-assembly. Not only are oligo(ethylene glycol) groups typically immiscible with hydrophobic *n*-alkyl chains, but they have been shown to exhibit favourable attractive interactions with imidazolium cations, especially at the weakly acidic proton on the C(2) position between the N(1) and N(3) positions [44]. Through weak H-bonding interactions, alkyl ether units may be actively aiding in the organisation of gemini imidazolium LC amphiphiles.

Figure 9 shows PLM optical textures observed for the SmA phases of the oligo(ethylene glycol)-bridged gemini imidazolium LCs. The focal conic texture present in Figure 9(d) is especially noteworthy. It was produced after annealing the sample at 120°C for 5 min and letting it slowly cool to 30°C. Figure 10 shows the corresponding powder XRD patterns associated with the respective thermotropic LC phases.

4. Conclusions

An initial library of 20 symmetric, imidazolium-based, gemini mesogens with long alkyl tails was synthesised. Fourteen of these salts displayed SmA thermotropic LC phases. Spacer length and the nature of the spacer group (*n*-alkyl vs. oligo(ethylene glycol)) were found to have the greatest influence over whether a thermotropic LC phase can be formed. Tail length also appeared to play a minor role in phase formation within the alkyl-bridged systems. Anion type was observed to have little or no effect on thermotropic LC phase formation, but it did have an influence on the temperature at which phase transitions occur for analogous compounds. Systems with longer alkyl tails were found to have larger *d*-spacings than those with the same spacer but shorter tails, providing some ability to control the dimensions of the SmA phase layer distance.

Gemini imidazolium ionic LCs represent a versatile platform for molecular design. Many opportunities exist to further explore their fundamental structure–property relationships to guide their potential future use as functional materials. Our next work will focus on examining the lyotropic LC behaviours of these ionic gemini compounds in water, polar organic solvents and ILs. Imidazolium-based nanocomposites may provide new opportunities for materials applications [45, 46] and serve as complements to the phosphonium-based LCs from which we have successfully constructed nanostructured materials [47–49].

Acknowledgements

Financial support for this research from the US Army Research Office (AB07CBT010), the Defense Threat Reduction Agency (HDTRA1-08-1-0028) and the National Science Foundation (DMR-0552399 and CBET-08054553) is gratefully acknowledged.

References

[1] Binnemans, K. *Chem. Rev.* **2005**, *105*, 4148–4204, and references therein.

[2] Wasserscheid, P., Welton, T. Eds. *Ionic Liquids in Synthesis*, 2nd ed.; Wiley-VCH: Weinheim, Germany, 2007.

[3] Menger, F.M.; Keiper, J. S. *Angew. Chem. Int. Ed.* **2000**, *39*, 1907–1920.

[4] In, M.; Zana, R. *J. Dispersion Sci. Technol.* **2007**, *28*, 143–154.

[5] Anderson, J.L.; Ding, R.; Ellern, A.; Armstrong, D.W. *J. Am. Chem. Soc.* **2005**, *127*, 593–604.

[6] Ding, Y.-S.; Zha, M.; Zhang, J.; Wang, S.-S. *Colloid Surface A* **2007**, *298*, 201–205.

[7] Huang, K.; Han, X.; Zhang, X.; Armstrong, D.W. *Anal. Bioanal. Chem.* **2007**, *389*, 2265–2275.

[8] Han, X.; Armstrong, D.W. *Org. Lett.* **2005**, *7*, 4205–4208.

[9] Wang, Y.; Marques, E.F. *J. Phys. Chem. B.* **2006**, *110*, 1151–1157.

[10] Sharma, V.; Borse, M.; Devi, S.; Dave, K.; Pohnerkar, J.; Prajapati, A. *J. Dispersion Sci. Technol.* **2005**, *26*, 421–427.

[11] Dreja, M. *Chem. Commun.* **1998**, *13*, 1371–1372.

[12] Baltazar, Q.Q.; Chandawalla, J.; Sawyer, K.; Anderson, J.L. *Colloid Surface A* **2007**, *302*, 150–156.

[13] Zeng, Z.; Phillips, B.S.; Xiao, J.-C.; Shreeve, J.M. *Chem. Mater.* **2008**, *20*, 2719–2726.

[14] Mingqi, A.; Guiying, X.; Yanyan, Z.; Yan, B. *J. Colloid Interface Sci.* **2008**, *326*, 490–495.

[15] Anderson, J.L.; Armstrong, D.W. *Anal. Chem.* **2005**, *77*, 6453–6462.

[16] Bara, J.E.; Hatakeyama, E.S.; Gabriel, C.J.; Zeng, X.; Lessmann, S.; Gin, D.L.; Noble, R.D. *J. Membr. Sci.* **2008**, *316*, 186–191.

[17] Nakajima, H.; Ohno, H. *Polymer* **2005**, *46*, 11499–11504.

[18] Carlisle, T.K.; Bara, J.E.; LaFrate, A.L.; Gin, D.L.; Noble, R.D. *J. Membr. Sci.* **2010**, *359*, 37–43.

[19] Tan, B.-H.; Yoshio, M.; Watanabe, K.; Hamasaki, A.; Ohno, H.; Kato, T. *Polym. Adv. Technol.* **2008**, *19*, 1362–1368.

[20] Yazaki, S.; Funahashi, M.; Kato, T. *J. Am. Chem. Soc.* **2008**, *130*, 13206–13207.

[21] Yazaki, S.; Kamikawa, Y.; Yoshio, M.; Hamasaki, A.; Mukai, T.; Ohno, H.; Kato, T. *Chem. Lett.* **2008**, *37*, 538–539.

[22] Shimura, H.; Yoshio, M.; Hoshino, K.; Mukai, T.; Ohno, H.; Kato, T. *J. Am. Chem. Soc.* **2008**, *130*, 1759–1765.

[23] Yoshio, M.; Ichikawa, T.; Shimura, H.; Harutoki, K.; Kagata, T.; Hamasaki, A.; Mukai, T.; Ohno, H.; Kato, T. *Bull. Chem. Soc. Jpn.* **2007**, *80*, 1836–1841.

[24] Yoshio, M.; Kagata, T.; Takayoshi, H.; Hoshino, K.; Mukai, T.; Ohno, H.; Kato, T. *J. Am. Chem. Soc.* **2006**, *128*, 5570–5577.

[25] Yoshio, M.; Mukai, T.; Ohno, H.; Kato, T. *J. Am. Chem. Soc.* **2004**, *126*, 994–995.

[26] Mukai, T.; Yoshio, M.; Kato, T.; Ohno, H. *Chem. Lett.* **2004**, *33*, 1630–1631.

[27] Hoshino, K.; Yoshio, M.; Mukai, T.; Kishimoto, K.; Ohno, H.; Kato, T. *J. Polym. Sci. Polym. Chem.* **2003**, *41*, 3486–3492.

[28] Chiou, J.Y.Z.; Chen, J.N.; Lei, J.S.; Lin, I.J.B. *J. Mater. Chem.* **2006**, *16*, 2972–2977.

[29] Lee, K.-M.; Lee, Y.-T.; Lin, I.J.B. *J. Mater. Chem.* **2003**, *13*, 1079–1084.

[30] Dobbs, W.; Douce, L.; Allouche, L.; Louati, A.; Malbosc, F.; Welter, R. *New J. Chem.* **2006**, *30*, 528–532.

[31] Suisse, J.-M.; Douce, L.; Bellemin-Laponnaz, S.; Maisse-Francois, A.; Welter, R.; Miyake, Y.; Shimizu, Y. *Eur. J. Inorg. Chem.* **2007**, *24*, 3899–3905.

[32] Goossens, K.; Nockemann, P.; Driesen, K.; Goderis, B.; Goerller-Walrand, C.; Van Hecke, K.; Van Meervelt, L.; Pouzet, E.; Binnemans, K.; Cardinaels, T. *Chem. Mater.* **2008**, *20*, 157–168.

[33] Kouwer, P.H.J.; Swager, T.M. *J. Am. Chem. Soc.* **2007**, *129*, 14042–14052.

[34] Trilla, M.; Pleixats, R.; Parella, T.; Blanc, C.; Dieudonne, P.; Guari, Y.; Man, M.W.C. *Langmuir* **2008**, *24*, 259–265.

[35] Kumar, S.; Pal, S.K. *Tetrahedron Lett.* **2005**, *46*, 2607–2610.

[36] Batra, D.; Hay, D.N.T.; Firestone, M.A. *Chem. Mater.* **2007**, *19*, 4423–4431.

[37] Batra, D.; Seifert, S.; Firestone, M.A. *Macromol. Chem. Phys.* **2007**, *208*, 1416–1427.

[38] Boydston, A.J.; Pecinovsky, C.S.; Chao, S.T.; Bielawski, C.W. *J. Am. Chem. Soc.* **2007**, *129*, 14550–14551.

[39] Zhai, X.; Liu, M. *J. Colloid Interface Sci.* **2006**, *295*, 181–187.

[40] Supporting Information published with reference 39.

[41] Blanton, T.N.; Huang, T.C.; Toraya, H.; Hubbard, C.R.; Robie, S.B.; Louër, D.; Göbel, H.E.; Will, G.; Gilles, R.; Raftery, T. *Powder Diffr.* **1995**, *10*, 91–95.

[42] Baxter, B.C.; Gin, D.L. *Macromolecules* **1998**, *31*, 4419–4425.

[43] Gray, G.W.; Goodby, J.W.G. *Smectic Liquid Crystals: Textures and Structures*; Leonard Hill: Glasgow, 1984.

[44] Smith, G.D.; Borodin, O.; Li, L.; Kim, H.; Liu, Q.; Bara, J.E.; Gin, D.L.; Noble, R.D. *Phys. Chem. Chem. Phys.* **2008**, *41*, 6301–6312.

[45] Gin, D.L.; Pecinovsky, C.S.; Bara, J.E.; Kerr, R.L. *Struct. Bond.* **2008**, *128*, 181–222.

[46] Gin, D.L.; Bara, J.E.; Noble, R.D.; Elliott, B.J. *Macromol. Rapid. Commun.* **2008**, *29*, 367–389.

[47] Lu, X.; Nguyen, V.; Zeng, X.; Elliott, B.J.; Gin, D.L. *J. Membr. Sci.* **2008**, *318*, 397–404.

[48] Zhou, M.; Nemade, P.R.; Lu, X.; Zeng, X.; Hatakeyama, E.S.; Noble, R.D.; Gin, D.L. *J. Am. Chem. Soc.* **2007**, *129*, 9574–9575.

[49] Pindzola, B.A.; Jin, J.; Gin, D.L. *J. Am. Chem. Soc.* **2003**, *125*, 2940–2949.